A COMPARATIVE STUDY OF TWO NUMERICAL METHODS FOR REGULATING UNSTEADY FLOW IN OPEN CHANNELS

دراسة مقارنة بين طريقتين عدديتين لتنظيم السريان الغير مستقر فى القنوات المكشوفة

M.T.Shamaa

Irrigation & Hydraulics Dept., Faculty of Engineering, Mansoura University, Egypt

خلاصة :

يمكن محاكاة السريان الغير مستقر فى القنوات المكشوفة بحل معادلات الحركة لسانت فنانت وذلك للتنبؤ بالتصرفات ومناسيب المياه فى القناة خلال الفترات الزمنية المقبلة تحت الاشتراطات المطلوبة. على الجانب الآخر تستخدم مسألة التشغيل لحساب التصرف الداخل أعلى القناة أو لحساب جدول التشغيل لقناطر نظام التوزيع وذلك للحصول على الاحتياجات المائية المطلوبة عند نهاية القناة. هذا النوع من المسائل يعرف أيضا بالحساب المعكوس للسريان فى القنوات المفتوحة. تم استخدام النموذج الرياضى الضمنى (implicit) للفروق المحدودة لبريسمان بتطبيق معادلات سانت فنانت لحل مسألة التشغيل فى القنوات المكشوفة. أظهرت النتائج المحسوبة لجميع الاختبارات العددية باستخدام النموذج الرياضى الضمنى للفروق المحدودة لبريسمان دقة اكبر وتذبذب أقل من تلك النتائج المحسوبة باستخدام النموذج الرياضى الصريح (explicit). تم تطبيق النموذج الرياضى الضمنى المعكوس للفروق المحدودة لبريسمان بنجاح على جزء ذى قطاعات غير منتظمة من ترعة المنصورية بين مدينة ميت غمر وقنطرة السنابط.

ABSTRACT

Unsteady flow in open channels can be simulated by solving the Saint Venant equations to predict the discharge and water level in the channel during the future time series under the given condition. On the other hand, the operation problem is used to compute the inflow at the upstream section of the channel or a schedule of operation for the regulating structures of the delivery system to get a predefined water demand at the downstream end of the channel. This type of problem is also known as the inverse computation of open channel flow. The finite difference Preissmann implicit model was used to solve the operation-type problems in open channels, based on the saint Venant equations. The final linear system of equations was solved by the double-sweep algorithm. The computed results using the finite difference implicit model showed more accuracy and less oscillation than that obtained by an explicit model for all the numerical tests. The finite difference Preissmann implicit model was successfully applied to a nonprismatic reach of El-Mansouria canal between Meit-Ghamer and Sanayet regulator.

INTRODUCTION

Unsteady open channel flow is governed by the Saint Venant equation, which express the principles of conservation of mass and momentum. Mathematical models of unsteady open channel flow are commonly built for engineering purposes[1,3,4,7] such as flood defence design, navigation, flood forecasting, dam-break analysis, and irrigation scheme control.

Operation along irrigation canals aim to maintain a hydraulic targeted state in order to achieve reliable and equitable water deliveries to users. Mathematical models were developed for operation-type problems [2,5,6,8,10] to predict the upstream inflow according to the prescribed downstream flow hydrograph. Any error in the inflow rate prediction can cause high water losses or the dissatisfaction of users.

A transient control technique, known as gate stroking [2,10], was used to set gate movements and upstream inflow according to the prescribed downstream flow hydrograph. The technique used the method of characteristics which is more complex and unwieldy. Easier solution for solving the unsteady open channel governing equations can be obtained using finite differences. Two finite difference algorithms have been recently proposed for solving the inverse problem. The first one is the implicit method[2]and the other is the explicit method [6].

Accepted November 6, 2002.

The inverse implicit finite difference Preissmann scheme was tested with numerical experiments. The computed results using the inverse implicit scheme was compared with that obtained by the explicit backward operation scheme presented in Liu, et al. 1992 [6]. The effects of Manning's roughness coefficient and the channel bed slope on the computed upstream inflow were examined. Also, the inverse implicit scheme was applied successfully to a nonprismatic reach of El-Mansouria canal between Meit-Ghamer and Sanayet regulator [9].

GOVERNING EQUATIONS

The continuity equation and the momentum equation which are used to describe open channel flow, usually referred to as de Saint Venant equations. The Saint Venant equations can be formulated in different ways, depending on the assumptions used in their derivations. Assuming no lateral outflow, these equations can be written as:

$$\frac{\partial y}{\partial t} + \frac{1}{b}\frac{\partial Q}{\partial x} = 0 \qquad (1)$$

$$\frac{\partial Q}{\partial t} + \frac{\partial}{\partial x}\left(\beta \frac{Q^2}{A}\right) + gA\left(\frac{\partial y}{\partial x} + S_f - S_0\right) = 0 \qquad (2)$$

where: A = wetted cross-sectional area; b = wetted top width; g = gravitational constant; Q = discharge (through A); y = depth of flow ; t = time; x = space; S_0= bottom slope of the channel and S_f = friction slope.

NUMERICAL SOLUTION METHODS

Numerical Solution of the Saint Venant equations can be obtained at a finite number of grid points in the rectangular spatial-time grid using finite difference methods [1,3,4,7]. Finite difference schemes can be classified into two types: explicit and implicit. In the explicit difference methods, the dependent variables, at a rectangular grid point on an advanced time line are determined from the known values and conditions at grid points on the present time line or present and previous time lines. In the implicit methods, unsteady flow may be obtained at a subsequent time levels on the x-t plane by setting up many equations as there are unknown dependent variables and by solving them simultaneously using appropriate time boundary conditions.

Preissmann Implicit Routing Model

Implicit schemes which can use large time steps without any stability problem are more widely applied. The Preissmann scheme is the most widely applied implicit finite difference method because of its simple structure with both flow and geometrical variable in each grid point [1,3,4,7]. This implies a simple treatment of boundary conditions and a simple incorporation of structure and bifurcation points. Also, it has the advantages that steep wave fronts may be properly simulated by varying the weighting coefficient.

The computational grid for the Preissmann implicit scheme is shown in Fig.1. The application of the Preissmann scheme to the derivatives in equations (1) and (2) yields,

$$\frac{\partial f}{\partial t} = \phi\frac{f_{j+1}^{n+1} - f_{j+1}^{n}}{\Delta t} + (1-\phi)\frac{f_j^{n+1} - f_j^{n}}{\Delta t} \qquad (3)$$

$$\frac{\partial f}{\partial x} = \theta \frac{f_{j+1}^{n+1} - f_j^{n+1}}{\Delta x} + (1-\theta) \frac{f_{j+1}^{n} - f_j^{n}}{\Delta x} \qquad (4)$$

$$f(x,t) = \theta\left[\phi f_{j+1}^{n+1} + (1-\phi) f_j^{n+1}\right] + (1-\theta)\left[\phi f_{j+1}^{n} + (1-\phi) f_j^{n}\right] \qquad (5)$$

where $f_j^n = f(j\Delta x, n\Delta t)$; Δx=space interval; Δt=time interval; ϕ = a weighting coefficient for distributing terms in space and θ = a weighting coefficient for distributing terms in time, $0 \le \theta \le 1$. In the above expressions, all the variables with subscripts' n are known and all the variables with subscripts' $n+1$ are the unknowns. Applying these numerical approximations to equations (1) and (2) yields

$$C\, y_j^{n+1} + D\, Q_j^{n+1} + E\, y_{j+1}^{n+1} + F\, Q_{j+1}^{n+1} + G = 0 \qquad (6)$$

$$C'\, y_j^{n+1} + D'\, Q_j^{n+1} + E'\, y_{j+1}^{n+1} + F'\, Q_{j+1}^{n+1} + G' = 0 \qquad (7)$$

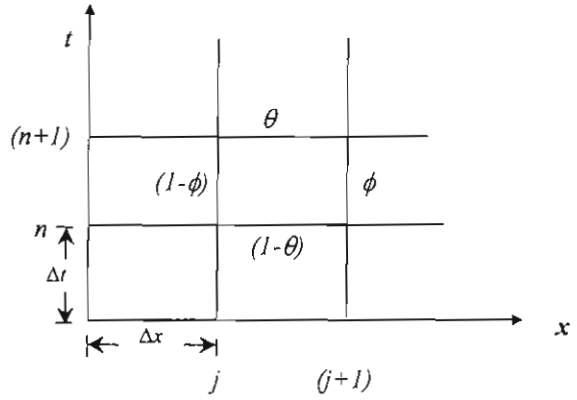

Fig. 1. Computational Grid for Preissmann Scheme

Where C, D, E, F, G, C', D', E', F', and G' are coefficients computed with known values at time level n. Equations (6) and (7) constitute a system of linear algebraic equations in four unknowns. As there are J points on the row $n+1$, there are $J-1$ rectangular grids and $J-1$ cells in the channel. Thus there are $2(J-1)$ equations for the evaluation of $2J$ unknowns. Two boundary conditions provide the necessary two additional equations to close the system. Any standard method of solving linear algebraic equations can be applied to obtain the solution of $2(J-1)$ equations. The double-sweep method [4,7] is very efficient and saves the time consumed by solution.

Explicit Backward Operation Method

For operation problems, the expected discharge and water level downstream boundary conditions are specified. The backward operation method [6] is an explicit solution based on the Preissmann scheme. Considering the time level (N) as the final condition (Fig. 2), and knowing Q_J , and y_J between any two time levels at the downstream section, the discharge and water depth profile at the time level $(N-1)$ can be computed by proceeding first backward in space and then backward in time. In this approach, the Preissmann scheme, Fig. 2, is written as:

$$\frac{\partial f}{\partial t} = \phi \frac{f_{j-1}^{n} - f_{j-1}^{n-1}}{\Delta t} + (1-\phi) \frac{f_{j}^{n} - f_{j}^{n-1}}{\Delta t} \quad (8)$$

$$\frac{\partial f}{\partial x} = \theta \frac{f_{j}^{n-1} - f_{j-1}^{n-1}}{\Delta x} + (1-\theta) \frac{f_{j}^{n} - f_{j-1}^{n}}{\Delta x} \quad (9)$$

$$f(x,t) = \theta\left[\phi f_{j-1}^{n-1} + (1-\phi) f_{j}^{n-1}\right] + (1-\theta)\left[\phi f_{j-1}^{n} + (1-\phi) f_{j}^{n}\right] \quad (10)$$

The solution begins at the top-right corner of the time-distance plane, Fig. 2. The application of the finite difference equations yields an algebraic system of two equations and two unknowns. The solution obtained cell by cell, moving first backward in space and then backward in time.

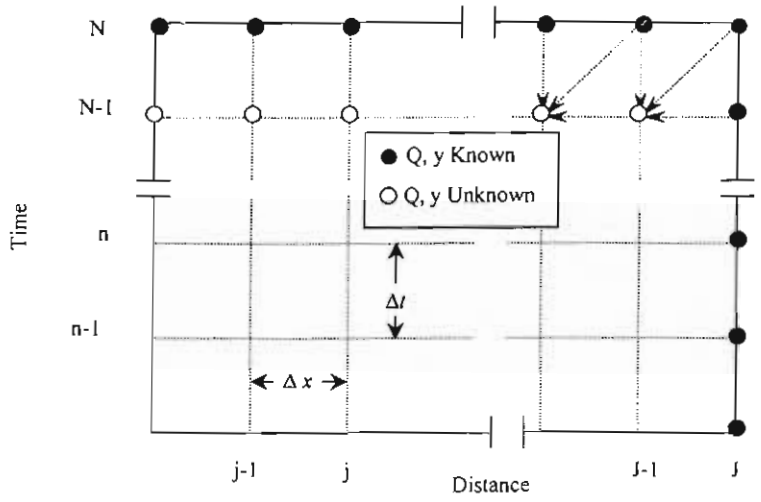

Fig. 2. Explicit Backward Computational Grid

Inverse Implicit Finite Difference Method

The computational scheme can be shown as a boundary value problem rotated 90° in the distance-time grid [2] as shown in Fig.3. The specified depths and discharges are the initial conditions in this rotated problem. The boundary condition can be either a discharge profile or water depth profile at both the initial time and the final computational time. The application of the Preissmann scheme to the derivatives in equations (1) and (2) yields the same equations (8), (9) and (10). The solution proceeds upstream by solving *2(N-1)* equations for the evaluation of *2N* unknowns. The two boundary conditions provide the necessary two additional equations to close the system.

DESCRIPTION OF TEST CANAL

The performance of the inverse implicit finite difference scheme was tested using the example presented in Liu, et al. 1992 [6]. The foregoing test is for the unsteady flow in a trapezoidal channel with a bottom width of *5.0m* and side slopes *1.5H to 1V*. The bottom slope is *0.001*, Manning's *n=0.025*, the channel length is *2.5km*, and a fixed overflow weir with free flow condition is considered as a downstream outlet. At the downstream outlet, the discharge increases from *5* m^3/sec to *10* m^3/sec in one hour, it remains constant at *10* m^3/sec for two

hours, then decreases to $5.0\ m^3/sec$ in one hour (demand line in Fig. 4.). The discharge-water depth relationship of a fixed weir under free-flow condition was used to obtain the water depth at the downstream end section. The discharge and water depth at the upstream intake, Figs. 4 and 5, were computed using the specified dischargc and water depth at the downstream end section as the initial condition.

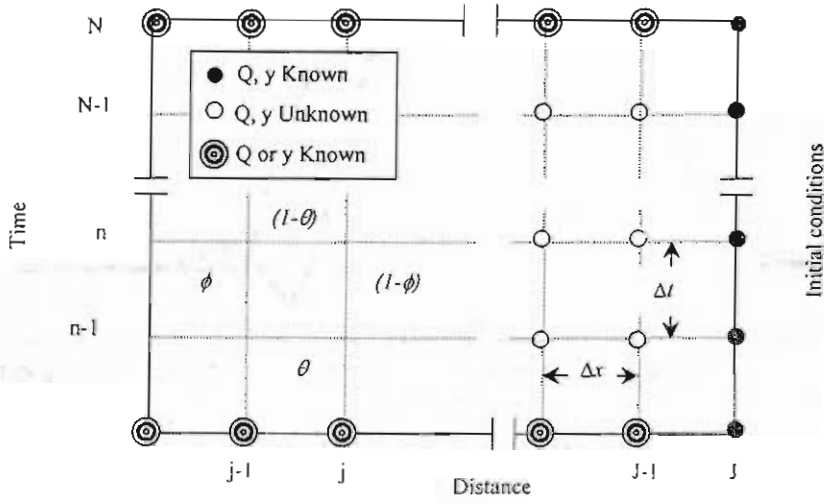

Fig. 3. Implicit Finite Difference Computational Grid

The obtained upstream discharge hydrograph was then used as upstream boundary condition and the fixed overflow weir at the end of the channel was used as the downstream boundary condition, to simulate the flow in the channel with the routing implicit finite difference scheme. The computed downstream hydrographs reasonably reproduced the prescribed demand, Figs. 4 and 5.

NUMERICAL TESTS AND COMPARISON OF RESULTS

The computed upstream discharge and depth hydrographs using both of the backward-operation explicit method and the inverse implicit method are shown in Figs. 4 and 5. The space interval $\Delta x = 500\ m$ and time interval $\Delta t = 300\ sec$ were used in both of the backward-operation explicit method and the inverse implicit method. The weighting coefficient $\phi = 0.5$ and the weighting coefficient $\theta = 1.0$ were used in the baekward-operation explicit method while the weighting coefficient $\phi = 1.0$ and the weighting coefficient $\theta = 0.8$ were used in the inverse implicit method. Figs. 4 and 5 show very little difference between the computed hydrographs using both the backward operation explicit method and the inverse implicit method. The upstream discharge hydrograph obtained by the inverse implicit scheme, when used as upstream boundary conditions in the routing problem, reproduced downstream flow hydrographs closer to what are expected.

The inverse implicit scheme was tested with numerical experiment by verifying the following parameters: The computation space interval Δx, the time interval Δt, the weighting coefficient ϕ, and the weighting coefficient θ The space interval $\Delta x = 250\ m$, the time interval $\Delta t = 100\ sec$, the weighting coefficient $\phi = 1.0$, and the weighting coefficient $\theta = 0.7$ were used in the computation of upstream hydrographs, except for the tested parameter.

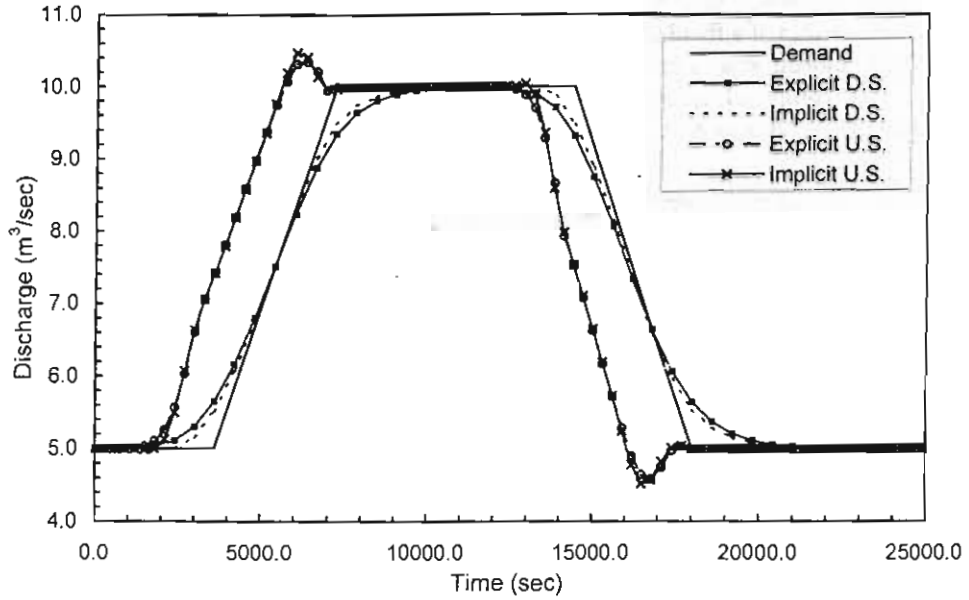

Fig. 4. Comparison between Discharge Hydrographs Using Explicit Backward Operation Method and Inverse Implicit Method.

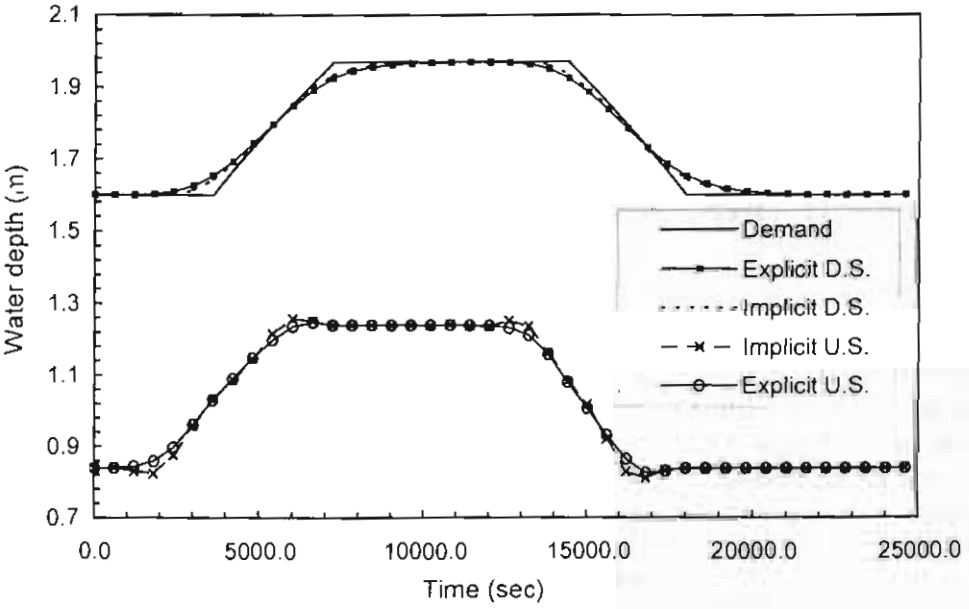

Fig. 5. Comparison between Water Depth Hydrographs Using Explicit Backward Operation Method and Inverse Implicit Method.

The computed upstream hydrographs using $\Delta x = 100\ m$, $250\ m$, and $500\ m$ are shown in Figs. 6 and 7. The computed hydrographs for $\Delta x = 100\ m$ show bigger oscillation during both the increasing and decreasing of the flow rate than the other two values. Figures 6 and 7 show that the increasing of Δx from $100\ m$ to $500\ m$ damped the oscillation during both the increasing and decreasing of the discharge. Liu et al.[6] showed that the effect of changing Δx has a little effect and could be neglected on computing the upstream hydrographs using the backward operation explicit method.

The computed upstream hydrographs, Figs.8 and 9, using $\Delta t = 60\ sec$, $600\ sec$, and $1200\ sec$ are shown in Figs.8 and 9. The time interval $\Delta t = 60\ sec$ shows more oscillation in the computed results during both the increasing and decreasing of the flow rate than that of the bigger values due to its superior accuracy. The computed results with time interval $\Delta t = 600\ sec$, and $1200\ sec$ show oscillation before the decreasing of flow from $10\ m^3/sec$ to $5.0\ m^3/sec$ which doesn't appear in the computed results with $\Delta t = 60\ sec$. Liu et al. 1992 [6] mentioned that the computed upstream hydrographs using the backward operation explicit method with a smaller time interval has more oscillation which can cause the failure of the computation, on the contrary to the inverse implicit finite difference scheme which has the advantage of stability.

Figures 10 and 11 show that the oscillations of the computed upstream hydrographs are damped as the weighting coefficient ϕ increases from 0.5 to 1.0. Bautista et al. [2] show the same effect of the weighting coefficient ϕ on the computed upstream discharge hydrographs for gate stroking problem. Liu et al. 1992 [6] didn't test the effect of the weighting coefficient ϕ on the computed hydrographs using the backward-operation explicit method.

The computed upstream hydrographs for different values of the weighting coefficient θ show that the oscillation during both the increasing and decreasing of the flow is damped when θ increases from 0.5 to 0.8, then the oscillations spread along the solution as θ increases from 0.8 to 1.0. Figs 12, and 13 show the computed upstream hydrographs for $\theta = 0.5$, 0.8, and 1.0. Bautista et al. [2] didn't test the effect of the weighting coefficient θ on the computed upstream discharge hydrographs for gate stroking problem. Liu et al. 1992 [6] showed a very big oscillation occurred on the upstream computed hydrographs, using the backward operation explicit method, for $\theta = 0.6$. This oscillation was damped as θ increased from 0.6 to 1.0.

The inverse implicit finite difference scheme was also tested using different channel length. As shown in Figs. 14 and 15, the length of the channel doesn't affect the oscillations of the computed upstream hydrographs, but the computed upstream hydrographs are more shifted to the left as the channel length increases to provide the same downstream flow pattern. Liu et al. 1992 [6] mentioned that the oscillations in the computed upstream discharge hydrographs using the backward operation explicit method are amplified with the increasing of channel length.

The effect of channel slope on the computed upstream hydrographs with the inverse implicit finite difference scheme was also tested using $S_0 = 0.001$, 0.0001, and 0.00001. The space interval $\Delta x = 500\ m$, the time interval $\Delta t = 200\ sec$, the weighting coefficient $\phi = 1.0$, and the weighting coefficient $\theta = 0.8$, were used in the computations. As shown in Figs. 16 and 17, for a channel length of $10\ km$, the damping effect of the finite difference Preissmann scheme is more visible as the bed slope of the channel becomes milder.

The effect of Manning's roughness coefficient on the upstream hydrographs for a channel length of $10\ km$ and a bottom slope of 0.001 was tested using $n = 0.025$, 0.02, and 0.015. The computed upstream discharge hydrograph shifts to the left as the Manning's roughness coefficient increases to provide the same downstream flow pattern. The computed upstream depth hydrograph shifts upward and to the left as the Manning's roughness coefficient increases. The results are shown in Figs. 18 and 19.

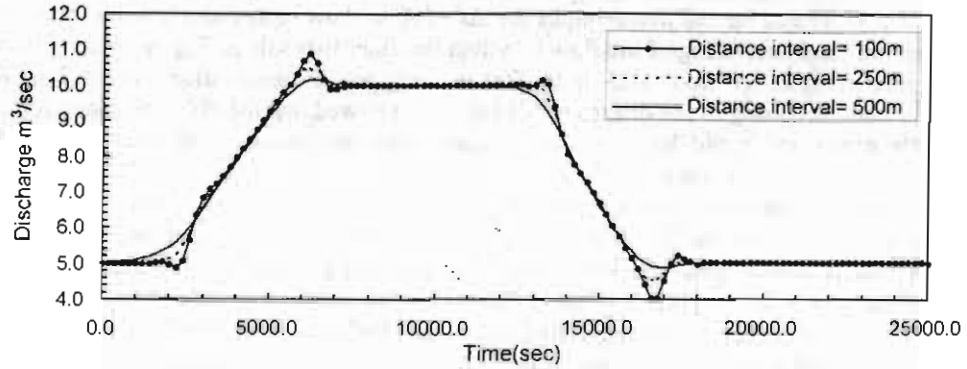

Fig. 6.Computed Upstream Discharge Hydrographs by Inverse Implicit Scheme at Different Distance Intervals.

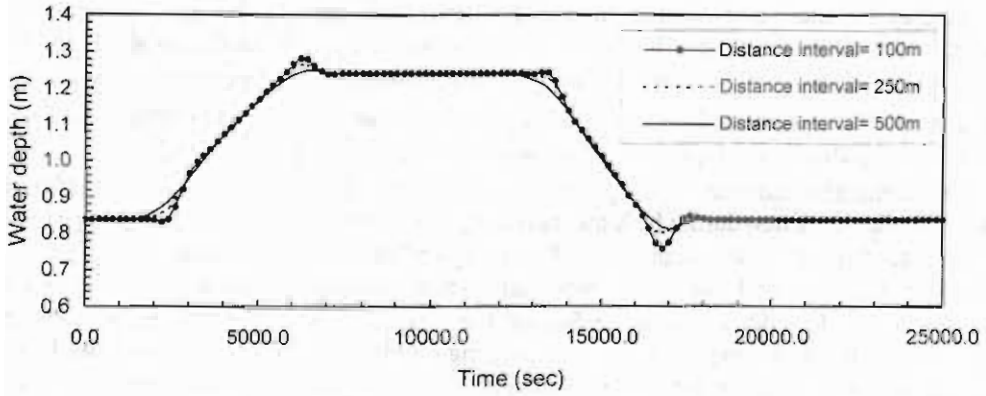

Fig. 7. Computed Upstream Water Depth Hydrographs by Inverse Implicit Scheme at Different Distance Intervals.

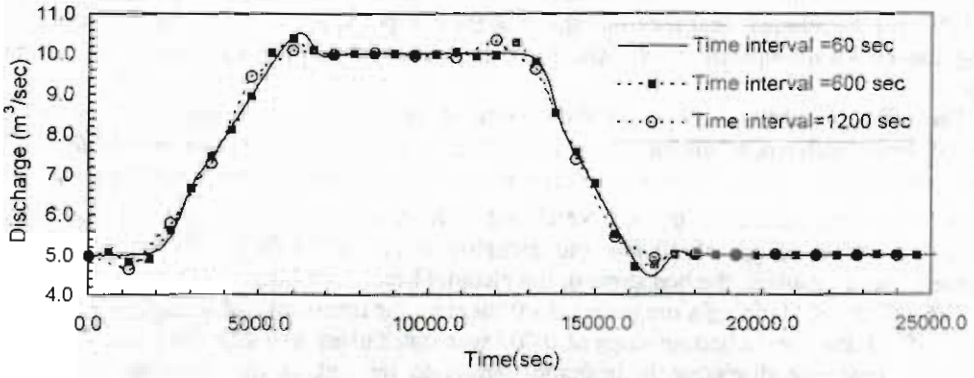

Fig. 8. Computed Upstream Discharge Hydrographs by Inverse Implicit Scheme at Different Time Intervals.

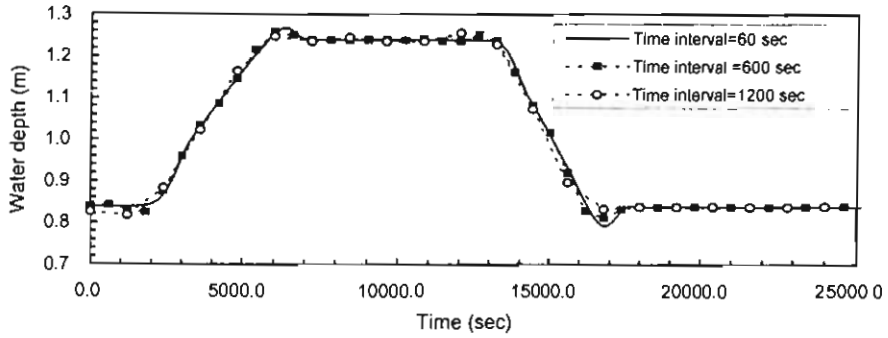

Fig. 9. Computed Upstream Water Depth Hydrographs by Inverse Implicit Scheme at Different Time Intervals.

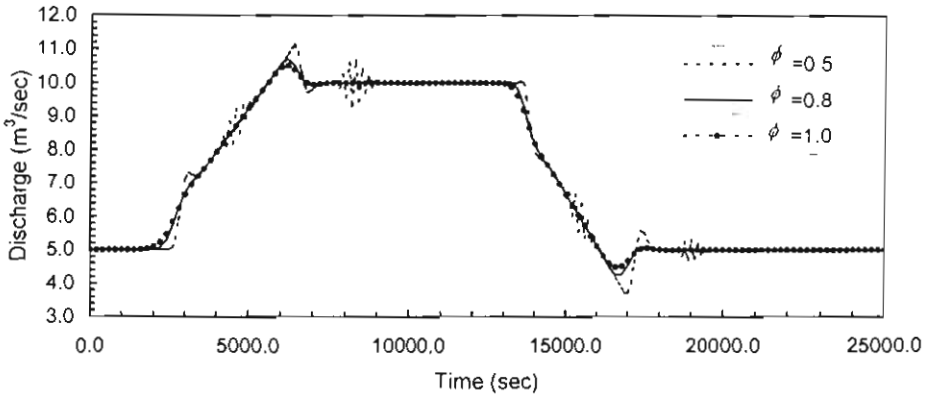

Fig. 10. Comparison of Computed Upstream Discharge Hydrographs Using Inverse Implicit Scheme with Different ϕ Factors.

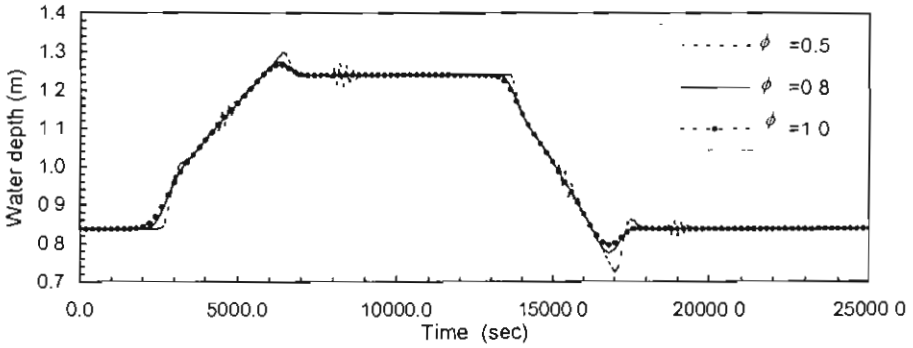

Fig. 11. Comparison of Computed Upstream Water Depth Hydrographs Using Inverse Implicit Scheme with Different ϕ Factors.

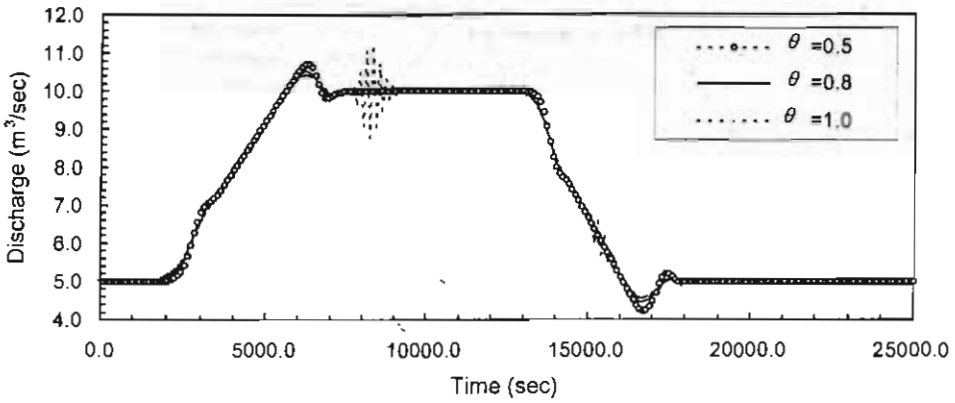

Fig. 12. Comparison of Computed Upstream Discharge Hydrographs Using Inverse Implicit Scheme with Different θ Factors.

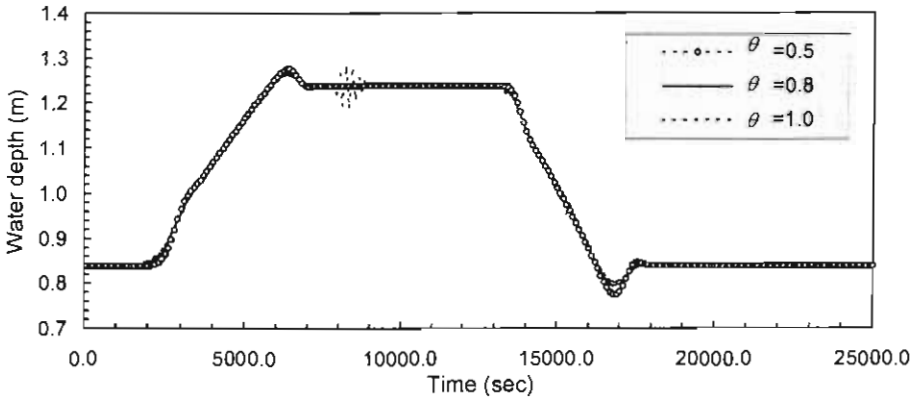

Fig. 13. Comparison of Computed Upstream Water Depth Hydrographs Using Inverse Implicit Scheme with Differentθ Factors.

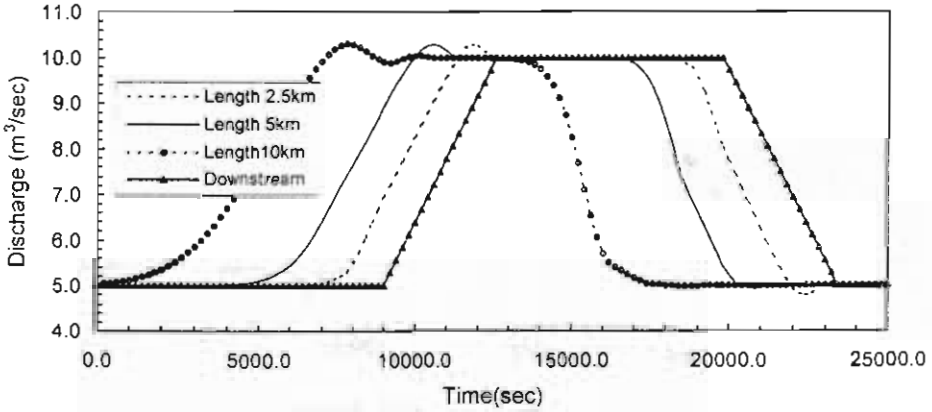

Fig. 14. Computed Upstream Discharge Hydrographs Using Inverse Implicit Scheme with Different Canal Lengths.

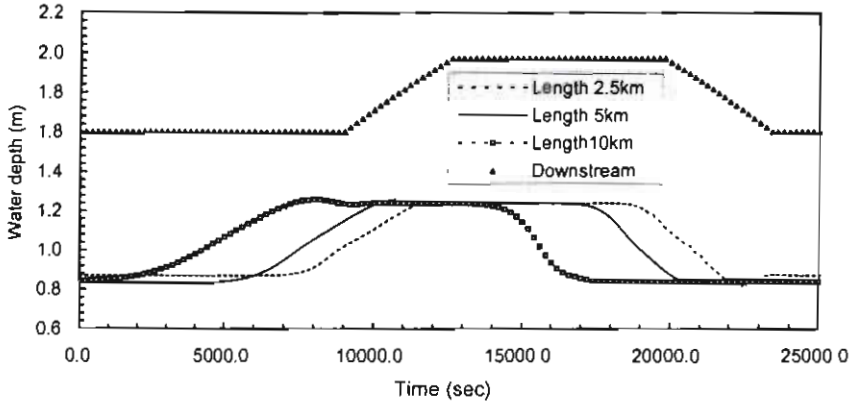

Fig. 15. Computed Upstream WaterDepth Hydrographs Using Inverse Implicit Scheme with Different Canal Lengths.

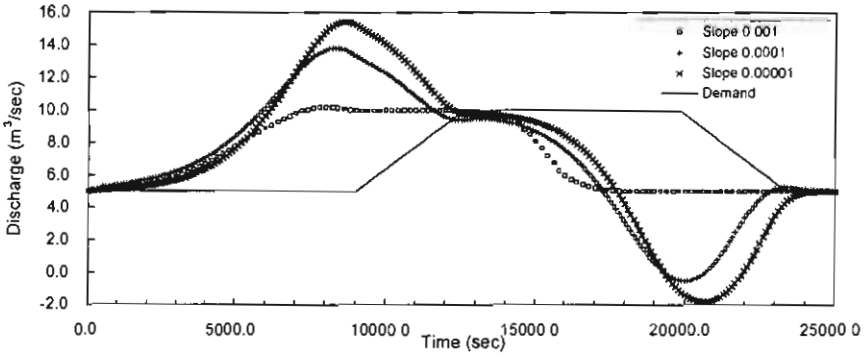

Fig. 16. Computed Upstream Discharge Hydrographs Using Inverse Implicit Scheme with Different Bed Channel Slopes.

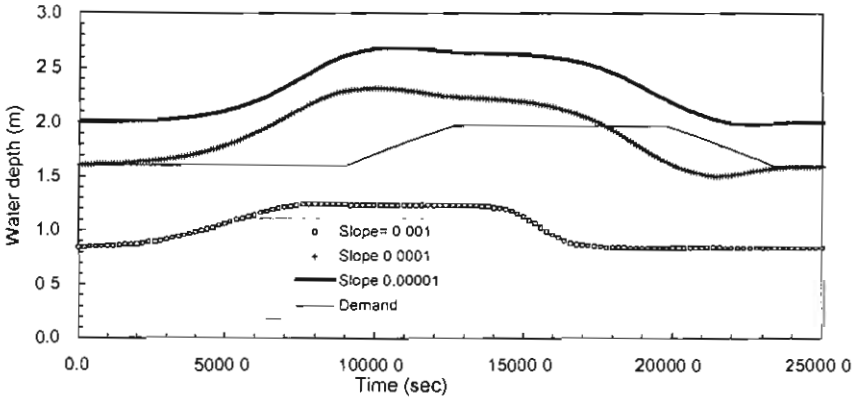

Fig. 17. Computed Upstream Water Depth Hydrographs Using Inverse Implicit Scheme with Different Bed Channel Slopes.

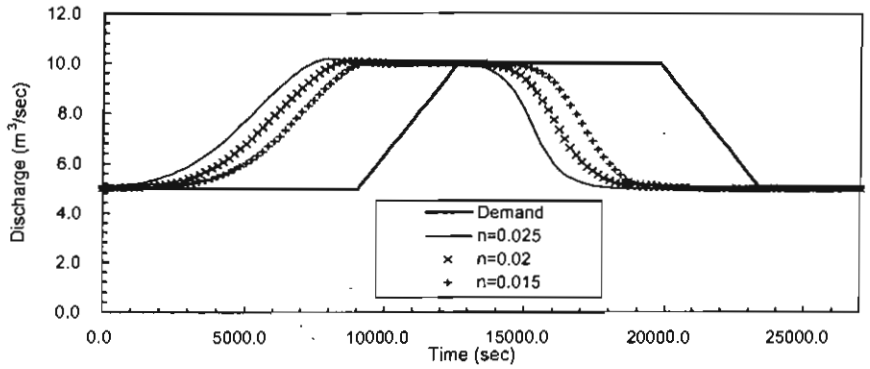

Fig. 18 . Computed Upstream Discharge Hydrographs for Different Manning's Roughness Coefficient.

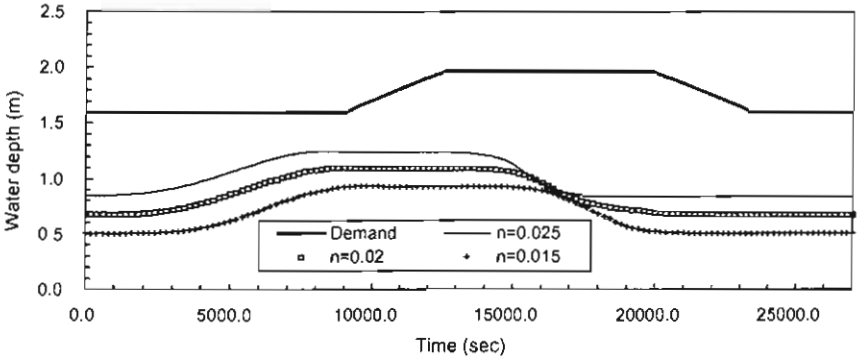

Fig. 19 . Computed Upstream Water Depth Hydrographs for Different Manning's Roughness Coefficient.

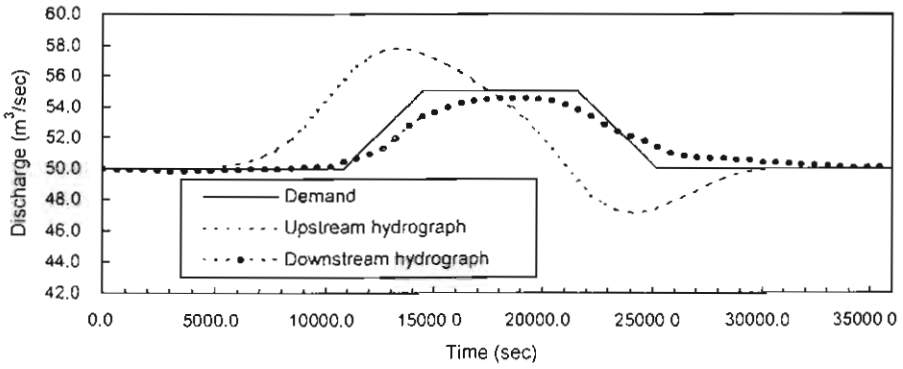

Fig. 20 . Computed Upstream Discharge Hydrograph Using Inverse Implicit Scheme for El-Mansouria Canal.

MODEL APPLICATION TO NON-PRISMATIC CHANNEL

The inverse implicit finite difference scheme was applied to a reach of El-Mansouria canal between Meit-Ghamer and Sanayat regulator. The length of this reach is *18 km*, the cross section spacing is *2.0 km*, the channel bed slope is *5.3 cm/km*, and the shape of the cross section is irregular [9]. At the downstream section, the discharge increases from *50 m^3/sec to 55 m^3/sec* in one hour, it remains at *55 m^3/sec* for two hours, then decreases to *50 m^3/sec* in one hour (demand line in Fig.20). The space interval $\Delta x = 2000\ m$, the time interval $\Delta t = 600\ sec$, the weighting coefficient $\phi = 1.0$, and the weighting coefficient $\theta = 0.6$, were used in the computations. The computed upstream discharge hydrograph is illustrated in Fig. 20. The damping effect of the finite difference Preissmann scheme is visible as shown in the computed upstream hydrograph due to the mild slope of the canal, Fig. 20. The computed upstream discharge hydrograph, when used as upstream boundary conditions in the routing problem of El-Mansouria canal, reproduced downstream discharge hydrograph closer to what is expected as shown in Fig. 20.

CONCLUSIONS

Two finite difference algorithms for regulating unsteady flow in open channel have been presented. The first one is the backward operation explicit method and the other is the inverse implicit finite difference method. The inverse implicit scheme was tested with the following parameters: the space interval Δx, the time interval Δt, the weighting coefficient ϕ, and the weighting coefficient θ.

The computed results, using the inverse implicit scheme, show small oscillation during both of the increasing and decreasing of the flow especially with the small space interval. The accuracy of computed results increases with decreasing of time interval. The oscillations of the computed upstream hydrographs are damped as the weighting coefficient ϕ increases from *0.5* to *1.0*. The oscillation of the computed upstream hydrographs during both of the increasing and decreasing of the flow rate is damped when θ increases from *0.5* to *0.8*, then the oscillations spread along the solution as θ increases from *0.8* to *1.0*.

The length of the channel doesn't affect the oscillations of the computed upstream hydrographs obtained with the inverse implicit scheme . The computed upstream hydrographs shift more to the left as the channel length increases to provide the same downstream flow pattern.

The effect of channel slope on the computed upstream hydrographs with the inverse implicit scheme was tested. The damping effect of the finite difference Preissmann scheme is more visible as the bed slope of the channel becomes milder.

The effect of Manning's roughness coefficient on the computation of upstream hydrographs was tested. The computed upstream discharge hydrograph shifts to the left as the Manning's roughness coefficient increases to provide the same downstream flow pattern. The computed upstream water depth hydrograph shifts upward and to the left as the Manning's roughness coefficient increases.

The computed results using the inverse implicit scheme was more accurate and show less oscillation than that obtained using the backward operation explicit method for all the cases of numerical tests. All the inverse solutions, when used as input to a routing model, produced downstream flow hydrographs very close to the required demand hydrographs.

REFERENCES

1. Abbott, M. B., "Computational Hydraulics; Elements of The Theory of Free Surface Flows", Pitman Publishing Limited, London, 1979.
2. Bautista, E., Clemmens, A.J., and Strelkoff, T. ," Comparison of Numerical Procedures for Gate Stroking", Journal of Irrigation and Drainage Engineering, ASCE, Vol.123, No.2, pp. 129-136, March/April,1997.
3. Chaudhry, M.H., "Open-Channel Flow", Prentice Hall, Inc., New Jersey, USA, 1993.
4. Cung, J.A., Holly, F.M. and Verwey, J.A. , "Practical Aspects of Computational River Hydraulics", Pitman Publishing Limited, London, 1980.
5. Schuurmans, W., "A Model to Study The Hydraulic Performance of Controlled Irrigation Canals", The Center for Operational Water Management, Delft University of Technology, 1991.
6. Liu, F., Feyen, J., and Barlamont, J., " Computational Method for Regulating Unsteady Flow in open channels.", Journal of Irrigation and Drainage Engineering, ASCE,Vol.118, No.10, pp. 674-689, September/October,1992.
7. Mahmood, K., and Yevjevich, "Unsteady Flow in Open Channels", Vol. I, Water Wylie, E. Resources Publications, 1975.
8. Reddy, J.M., Dia, A., and Oussou, A., "Design of Control Algorithm for Operation of Irrigation Canals", Journal of Irrigation and Drainage Engineering, ASCE,Vol.118, No.6, pp. 852-867, November/December,1992.
9. Shamaa, M. T., "Application of Resistance Formulae in Irrigation canals", M.Sc. Thesis, Civil Engineering Dept., El Mansoura University, Egypt, 1989.
10. Wylie, E. B., "Control of Transient Free Surface Flow" Journal of Hydraulic Engineering, ASCE, Vol. 95, No. 1, pp. 347-361, 1969.

NOTATION

The following symbols are used in this paper:

A = wetted cross-sectional area;
b = wetted top width;
f = general function;
g = gravitational constant;
j = cross-section index;
n = time-level index; Manning's coefficient;
Q = discharge (through A);
S_0 = bottom slope of the channel;
S_f = friction slope;
t = time;
x = space;
y = depth of flow ;
Δt = time interval;
Δx = space interval;
ψ = a weighting coefficient for distributing terms in space; and
θ = a weighting coefficient for distributing terms in time.